

# Research on stress corrosion behavior of CCSE40 welded by underwater wet welding with austenitic welding rod in seawater

Y Zou<sup>1</sup>, Q Bai<sup>1,2,\*</sup>, S Dong<sup>2</sup>, Z L Yang<sup>1</sup> and Y Gao<sup>1</sup>

<sup>1</sup> Shandong Provincial Key Laboratory of Ocean Environment Monitoring Technology, Institute of Oceanographic Instrumentation, Shandong Academy of Science. 28 Zhejiang Road, Qingdao, China.

<sup>2</sup> Ocean University of China, Qingdao, China

**Abstract.** The stress corrosion behavior of CCSE40 welded by underwater wet welding with austenitic welding rod in seawater was studied. Microstructure, mechanical property and stress corrosion cracking susceptibility of the underwater wet welding joint were analyzed by metallographic observation, tensile and bending tests, slow strain rate test (SSRT) and SEM. The results indicated that the weld zone (WZ) and the heat affected zone (HAZ) were all sensitive to the stress corrosion, and the WZ was more sensitive than the HAZ.

## 1. Introduction

Affected by the water environment, the arc of underwater wet welding for water thermal decomposition can cause hydrogen content in the weld bath in water much larger than that in air (up to 62-68%). The hydrogen partial pressure is higher, so that there is a lot of hydrogen in the weld tissue, about 30-40 ml/100 g, maximum up to 60-70 ml/100 g. This is several more times than that in air when welding with acidic electrodes. The high hydrogen content and fast cooling rate lead to the poor plasticity and toughness of the underwater wet welding joints, which exacerbates the cold crack formation and seriously affects the service safety of the underwater wet welding on ocean engineering structures [1, 2].

Hydrogen plays a major role in the stress corrosion. The content of hydrogen in the metal exceeding the allowable value can generate cracks and pores, which cause hydrogen embrittlement in the weld. It can result in hydrogen cracking, and eventually destroy the structure.

In the hydrogen-induced cracking study, the accurate determination of hydrogen concentration is significant. The hydrogen-induced cracking sensitivity of high-strength steel is closely related to the hydrogen concentration in the steel. The higher the hydrogen concentration, the stronger the sensitivity of hydrogen-induced cracking. Takagi et al. [4] have evaluated the hydrogen-induced cracking sensitivity of high strength steel materials with critical hydrogen diffusion concentrations. Nevertheless, due to the difficulty of the accurate determination of the hydrogen concentration in material, there is little report on the quantitative relationship between hydrogen concentration and material strength index. Akhurst [5] used the local hydrogen pressure to replace the hydrogen concentration in the material. Zielinski [6] studied the effect of the cathodic polarization on the mechanical properties of carbon steel, high strength steel and high strength low alloy steels in artificial seawater, and used linear regression analysis to indicate the relationship between the hydrogen-induced cracking sensitivity and the amount of hydrogen related. In recent years, with the rapid development of detection and measurement



technology, many new test methods have been applied, such as TGA-MS technology and TDS (Thermal Desorption Spectrometry) hydrogen measurement technology. TDS technology can improve the measurement accuracy of hydrogen concentration in high strength steel up to  $10^{-8}$  (0.01 wppm), which plays a very important role in the quantitative study of hydrogen induced cracking of high strength steel and the mechanism of hydrogen induced cracking [7-9]. Wang [10-12] used TDS technology and SSRT methods to study the quantitative relationship between the notch tensile strength of the high strength steel and the hydrogen content. The results showed that the diffusible hydrogen led to the decrease of the tensile strength of the high strength steel, and the degree of decrease was exponentially related to the content of the diffusible hydrogen, while the non-diffusible hydrogen had no effect on the hydrogen cracking. Jayalakshmi [13] used TGA-MS technique to accurately derive the nonlinear relationship between the hydrogen concentration and the hydrogen charging time.

There is no consensus on the mechanism of hydrogen embrittlement. The common view of the various theories is that the hydrogen atoms are induced by stress-induced diffusion to the high stress site. When the hydrogen is concentrated to the critical value, the fracture stress of the material decreases and breaks. It is not clear how the aggregated hydrogen works. Hydrogen embrittlement is a complex process of the interaction of multiple mechanisms. Researchers used different mechanisms to explain the observed phenomena. There is no mechanism to explain the hydrogen induced cracking in all environments.

In this paper, the microstructure and mechanical properties of CCSE40 welded by underwater wet welding with austenitic welding rod were studied. The sensitivity of stress corrosion was evaluated by slow strain rate test (SSRT) and scanning electron microscopy (SEM). The fracture mechanism of welded joint was analyzed.

## 2. Experimental materials and methods

The material under investigation was CCSE40 high strength low-alloy steel plate with 45° V-shape of the weld pool by underwater manual welding. The filler material was austenitic stainless steel electrode. The chemical composition of base metal (BM) and weld zone (WZ) are given in Tables 1. Multi-pass welding was applied to complete the joint. The underwater welding was carried out in a tank, of which the size was 2 m×3 m×3 m. The tank was filled with seawater, the depth of which was 2 m.

**Table 1.** Chemical compositions of base metal and WZ of CCSE40 steel (mass fraction / %)

Position	C	Mn	Si	S	P	Mo	Ni	Cr	Fe
BM	0.18	1.2	0.50	0.035	0.035	0.08	0.40	0.20	Bal.
WZ	0.10	1.6	0.78	0.020	0.020	4.5	22.5	20.6	Bal.

Metallographic observations were carried out using GX51 Olympus metallurgical microscopy. A 10×30×10 mm specimen was obtained from the welded plate which composed of the BM, the WZ and the heat affected zone (HAZ). After ground with the SiC abrasive paper and polished to a mirror finish (1μm), this weldment sample was immersed into the etching solution. Because of different corrosion resistance, two etchants were used to reveal the microstructure of the joint. The etching of BM and HAZ was carried out using 3% Nital solutions (3 ml nitric acid (HNO<sub>3</sub>) 97 ml ethanol) then the microstructure of WZ was etched by the solution made of 5g CuSO<sub>4</sub>, 20ml hydrochloric acid and 20ml distilled water.

The fracture morphologies of the WZ, HAZ and BM for the underwater wet welding joint after SSRT were carried out using Philips XL30 scanning electron microscope.

The tensile and bending tests were carried out by universal testing machine. A cuboid specimen with 220×12×10 mm was taken along the vertical direction of the weld for the tensile test, while a cuboid specimen with 150×12×10 mm for the bending test. After cutting, the specimen was polished with metallurgical paper up to No.800 grade. The speeds of the tensile and the bending tests were 1 mm/min and 2 mm/min separately.

The size of SSRT sample is shown in Figure 1. The unit is mm. The coupons were polished with metallurgical paper up to No.1000 grade and cleaned with acetone. The slow strain rate tensile testing

machine was used for stress corrosion test. The rate was 0.002 mm/min. The test solution was natural seawater.

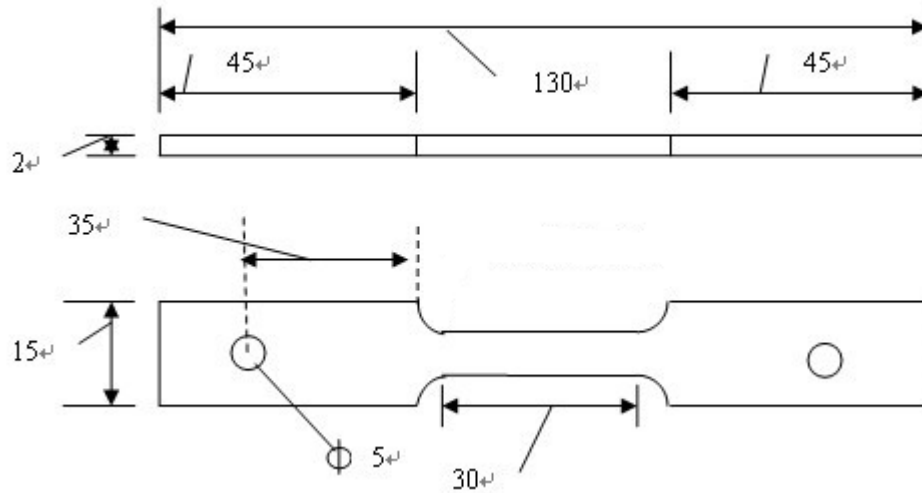


**Figure 1.** SSRT sample

### 3. Results and discussion

#### 3.1 Microstructure analysis

Figure 2 shows the microstructures of the fusion zone and the WZ. The top and the bottom of the picture are the near-fused line of the weld and the coarse zone of the HAZ. The coarse zone of the HAZ had a martensite structure, while the near-fused line of the weld had a sorbite and ferrite structure. As can be seen from Figure 2a, there was a crack parallel to the fused line in the coarse region of the HAZ, which was a hydrogen delayed crack. Under the effect of large heat input, the coarse zone of the HAZ overheating produced coarse grain. Under the condition of water cooling, the hardened martensite structure was formed. In combination of the constraints of the bottom plate and the hydrogen diffusion enrichment, the delayed crack formed. It was cold crack. Figure 2b shows a weld metal picture, and a crystal crack formed along a columnar grain boundary can be observed.

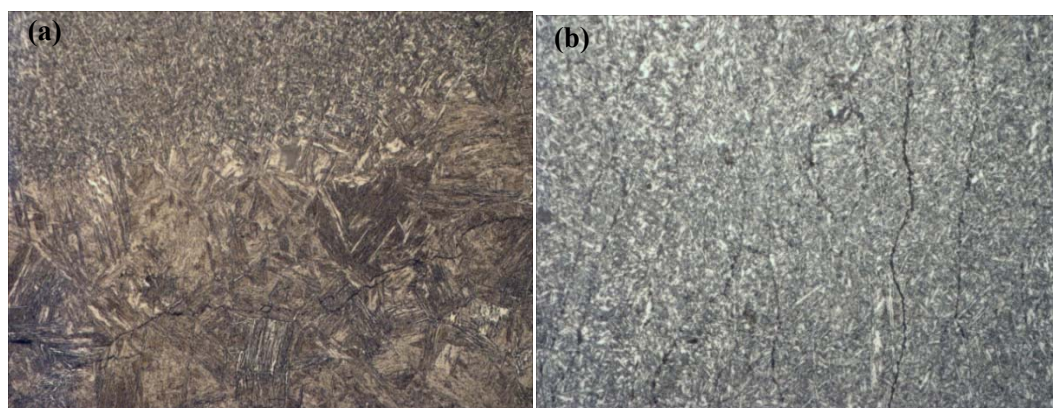


**Figure 2.** Microstructures of the weld joint (a) the fusion zone, (b) the WZ

#### 3.2 Mechanical property test

The mechanical properties of the underwater wet welding joint of austenitic electrode are shown in Table 2. The face bending of the coupon did not break, while the back bending cracked along the zone near the HAZ and the fusion line. The tensile coupon, without exception, spread along the HAZ and the

fused line to the weld (Figure 3). The tensile strength of the weld is higher than that of the base metal. The reason is that the hydrogen-induced cracking of the heat-affected zone leads to a decrease in the mechanical properties near the heat-affected zone.

**Table 2.** Mechanical properties of the underwater wet welding joint

Tensile properties of the welding joint			Tensile properties of the weld metal		Bending properties of the welding joint
Average tensile strength (MPa)	Average yield strength (MPa)	Fracture position	Tensile strength (MPa)	Elongation (%)	
509.9	401.4	Near the HAZ and the fused line	512.4	1.7	Face bending passed through. Back bending began to crack at 20°

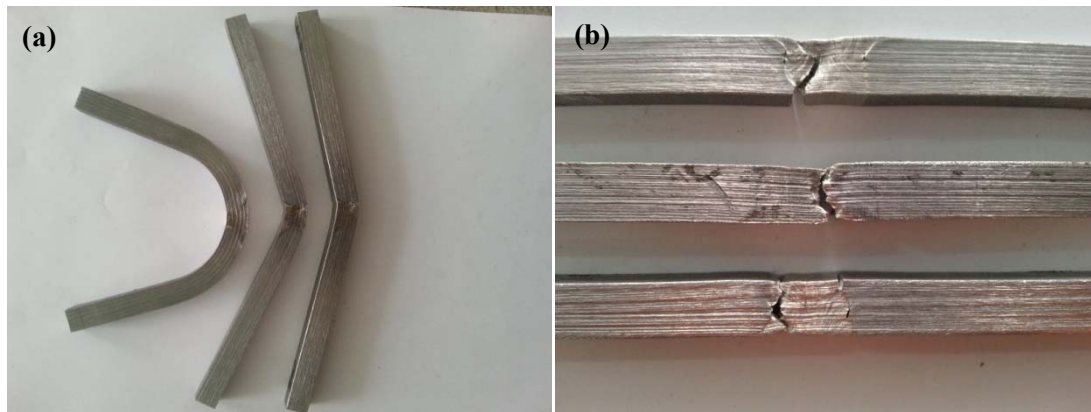


**Figure 3.** Morphologies of the underwater wet welding with austenitic welding rod after mechanical property test (a) bending test, (b) tensile test

### 3.3 Slow strain rate test (SSRT)

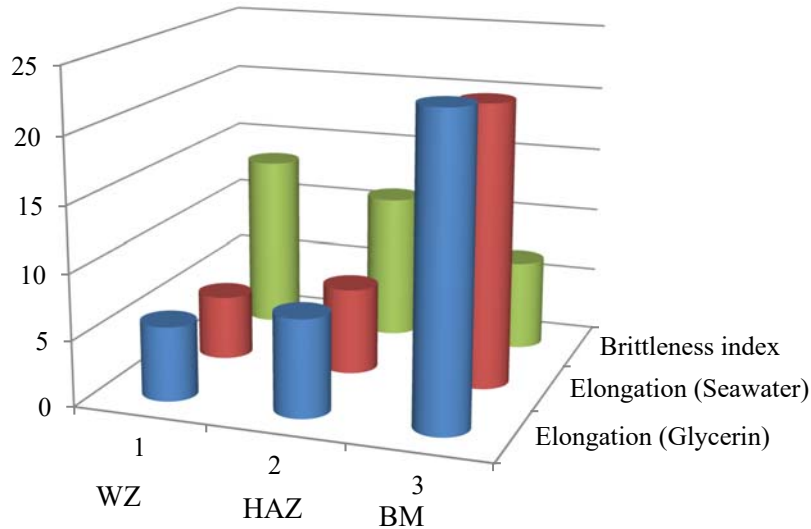
SSRT is of great significance in evaluating the stress corrosion cracking susceptibility of materials. As the test is in the indoor environment, the effects of other factors such as temperature, electrode potential and pH on the corrosion process can be studied simultaneously during SSRT. When the crack-free samples are slowly tensile failure in a specific medium and inert medium separately, according to the elongation  $\delta$ , the contraction of area  $\psi$ , the fracture time  $t_f$ , the absorbing energy, the fracture morphology, the characteristics of the secondary crack and other parameters to evaluate the materials stress corrosion cracking susceptibility.

The severity of stress corrosion cracking is usually related to the strain rate. If the strain rate is very large, the ductile fracture occurs before the material producing the effective stress corrosion cracking. On the contrary, if the strain rate is very small, the film breaks and repassivation follows, so that the crack tip exposed metal is too late to produce corrosion reaction. That is to say, it cannot produce stress corrosion cracking, but can produce a ductile fracture. The lower the strain rate, the lower the elongation, the longer the breaking time requires, the longer the time it need in the medium.

The relative difference ( $I$ ) between the elongation ( $\delta$ ) in the inertia medium and that in the corrosive medium or between the contraction of area ( $\psi$ ) in these two mediums are taken as a measurement of the stress corrosion susceptibility. That is  $I_\delta = (\delta_a - \delta_c) / \delta_a$  or  $I_\psi = (\psi_a - \psi_c) / \psi_a$ . Where “a” denotes the inert medium and “c” denotes the corrosive medium. The larger the  $I_\delta$  or  $I_\psi$ , the more sensitive to the stress corrosion.

The elongations for the BM, WZ and HAZ by SSRT in seawater and glycerin as well as the brittleness index which reflects the stress corrosion susceptibility are shown in Figure 4. As can be seen from the

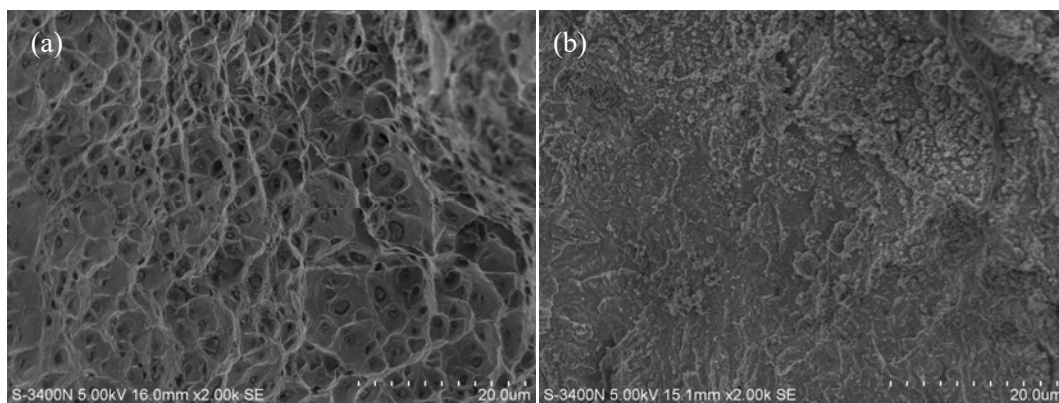
picture that the WZ and the HAZ were all sensitive to the stress corrosion. The weld was the most sensitive one, while the base metal was the most insensitive one. In seawater, the weld was the most susceptible to the stress corrosion.



**Figure 4.** SSRT results for the underwater wet welding in seawater

### 3.4 Scanning electron microscopy (SEM)

Figure 5 shows the fracture morphologies of the WZ, HAZ and BM for the underwater wet welding joint in seawater after SSRT. It can be seen from the picture that the WZ and the BM were ductile fracture, while the HAZ was quasi-cleavage fracture. The dimple center of the weld had a mixed phase. There were a large number of typical tectonic-shaped secondary cracks on the main fracture surface, which indicated that there was a hydrogen embrittlement mechanism for the underwater wet welding joints in seawater.



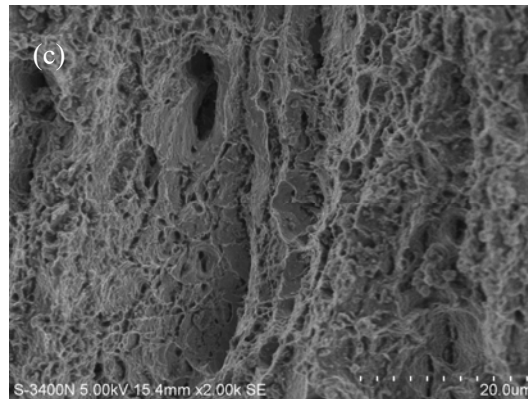


**Figure 5.** Fracture morphologies of the WZ, HAZ and BM for the underwater wet welding joint in seawater after SSRT (a) WZ, (b) HAZ, (c) BM

#### 4. Conclusion

(1) The coarse zone of the HAZ had a martensite structure, while the near-fused line of the weld had a sorbite and ferrite structure. There was a crack parallel to the fused line in the coarse region of the HAZ, which was a hydrogen delayed crack.

(2) The mechanical properties of the underwater wet welding joint of austenitic electrode showed that the back bending cracked along the zone near the HAZ and the fusion line. The tensile coupon spread along the HAZ and the fused line to the weld.

(3) From the SSRT results, the weld was the most sensitive to the stress corrosion, while the base metal was the most insensitive.

(4) The fracture morphologies showed that the WZ and the BM were ductile fracture, while the HAZ was quasi-cleavage fracture.

#### Acknowledgement

The authors appreciate the financial support by National Natural Science Foundation of China (No. 50971118) and National High-Tech Research & Development Program of China (No. 2008AA092901)

#### References

- [1] Yu J R, Zhang Y L and Jiang L P 2001 *Weld. Technol.* **30** 2
- [2] Ma C Y, Zhao J W and Song W Q 2007 *Proceedings of the 13th China Ocean (Shore) Engineering Symposium* 659
- [3] Li H L, Yu Z H, Li Y, Chu W Y and Qiao L J 2009 *Corros. Prot.* **30** 678
- [4] Takagi S, Inoue T, Hara T and Takahashi T 2000 *Tetsu-to-Hagane* **86** 689
- [5] Akhurst K N and Baker T J 1985 *Metall. Trans. A* **12** 1059
- [6] Zielinski A and Domzalicki P 2003 *J. Mater. Process. Tech.* **133** 230
- [7] Wei F G, Hara T, Tsuchida T and Tsuzaki K 2003 *ISIJ International* **43** 539
- [8] Nagumo M 1985 *Mater. Sci. Technol.* **1** 711
- [9] Wang M Q, Akiyama E and Tsuzaki K 2006 *Mater. Sci. Forum* **512** 55
- [10] Wang M Q, Akiyama E and Suzaki K 2005 *Scripta Mater.* **53** 713
- [11] Wang M Q, Akiyama E and Tsuzaki K 2005 *Scripta Mater.* **2** 403
- [12] Wang M Q 2006 *Trans. Mater. and Heat Treat.* **27** 57
- [13] Jayalakshmi S, Kim K B and Fleury E 2006 *J. Alloys Compd.* **417** 195
- [14] Yau T L 1982 *Corrosion* **38** 615
- [15] Lyle F F and Norris E B 1978 *Corrosion* **34** 193
- [16] Turn J C, Wilde B E and Troianos C A 1983 *Corrosion* **39** 364